frontiers in Marine Science

ORIGINAL RESEARCH
published: 22 May 2015
doi: 10.3389/fmars.2015.00026

Macroalgal responses to ocean acidification depend on nutrient and light levels

Paula S. M. Celis-Plá[1,2], Jason M. Hall-Spencer[3], Paulo Antunes Horta[4], Marco Milazzo[5], Nathalie Korbee[1], Christopher E. Cornwall[6,7] and Félix L. Figueroa[1]*

[1] Department of Ecology, Faculty of Science, University of Málaga, Málaga, Spain, [2] Laboratory of Botany, Faculty of Pharmacy, University of Barcelona, Barcelona, Spain, [3] Marine Biology and Ecology Research Centre, Plymouth University, Plymouth, UK, [4] Department of Botany, University Federal of Santa Catarina, Florianopolis, Brazil, [5] Dipartimento di Scienze della Terra e del Mare, University of Palermo, Palermo, Italy, [6] Institute for Marine and Antarctic Studies, University of Tasmania, Hobart, TAS, Australia, [7] School of Earth and Environment and ARC Centre of Excellence for Coral Reef Studies, University of Western Australia, Crawley, WA, Australia

OPEN ACCESS

Edited by:
Iris Eline Hendriks, University of the Balearic Islands, Spain

Reviewed by:
Peng Jin, King Abdullah University of Science and Technology, Saudi Arabia
Dorte Krause-Jensen, Aarhus University, Denmark

***Correspondence:**
Paula S. M. Celis-Plá, Department of Ecology, Faculty of Science, University of Málaga, Campus teatinos s/n, 29016 Málaga, Spain
paulacelispla@uma.es

Specialty section:
This article was submitted to Global Change and the Future Ocean, a section of the journal Frontiers in Marine Science

Received: *05 March 2015*
Accepted: *04 May 2015*
Published: *22 May 2015*

Citation:
Celis-Plá PSM, Hall-Spencer JM, Horta PA, Milazzo M, Korbee N, Cornwall CE and Figueroa FL (2015) Macroalgal responses to ocean acidification depend on nutrient and light levels. Front. Mar. Sci. 2:26. doi: 10.3389/fmars.2015.00026

Ocean acidification may benefit algae that are able to capitalize on increased carbon availability for photosynthesis, but it is expected to have adverse effects on calcified algae through dissolution. Shifts in dominance between primary producers will have knock-on effects on marine ecosystems and will likely vary regionally, depending on factors such as irradiance (light vs. shade) and nutrient levels (oligotrophic vs. eutrophic). Thus experiments are needed to evaluate interactive effects of combined stressors in the field. In this study, we investigated the physiological responses of macroalgae near a CO_2 seep in oligotrophic waters off Vulcano (Italy). The algae were incubated *in situ* at 0.2 m depth using a combination of three mean CO_2 levels (500, 700–800 and 1200 μatm CO_2), two light levels (100 and 70% of surface irradiance) and two nutrient levels of N, P, and K (enriched vs. non-enriched treatments) in the non-calcified macroalga *Cystoseira compressa* (Phaeophyceae, Fucales) and calcified *Padina pavonica* (Phaeophyceae, Dictyotales). A suite of biochemical assays and *in vivo* chlorophyll *a* fluorescence parameters showed that elevated CO_2 levels benefitted both of these algae, although their responses varied depending on light and nutrient availability. In *C. compressa*, elevated CO_2 treatments resulted in higher carbon content and antioxidant activity in shaded conditions both with and without nutrient enrichment—they had more Chl*a*, phenols and fucoxanthin with nutrient enrichment and higher quantum yield (F_v/F_m) and photosynthetic efficiency (α_{ETR}) without nutrient enrichment. In *P. pavonica*, elevated CO_2 treatments had higher carbon content, F_v/F_m, α_{ETR}, and Chl*a* regardless of nutrient levels—they had higher concentrations of phenolic compounds in nutrient enriched, fully-lit conditions and more antioxidants in shaded, nutrient enriched conditions. Nitrogen content increased significantly in fertilized treatments, confirming that these algae were nutrient limited in this oligotrophic part of the Mediterranean. Our findings strengthen evidence that brown algae can be expected to proliferate as the oceans acidify where physicochemical conditions, such as nutrient levels and light, permit.

Keywords: ocean acidification, macroalgae, photosynthesis, phenolic compounds, nutrient availability

Introduction

Ocean acidification due to increased atmospheric CO_2 levels is altering the concentrations of dissolved inorganic carbon (DIC) in surface waters; CO_3^{2-} levels are falling, which is expected to corrode marine carbonates, whilst CO_2 and HCO_3^- levels are rising which can stimulate photosynthesis (Connell et al., 2013; Cornwall et al., 2015). As some primary producers are better able to capitalize on increasing carbon availability than others, this is expected to alter marine communities (Hepburn et al., 2011; Connell et al., 2013; Koch et al., 2013; Gaylord et al., 2015). In the Mediterranean, surveys of coastal CO_2 seeps have repeatedly shown that coralline algae and sea urchins become less common as pH and CO_3^{2-} fall, whereas brown algae, such as *Cystoseira* spp., *Dictyota* spp., *Sargassum vulgare* and *Padina pavonica,* proliferate as CO_2 and HCO_3^- levels rise (Porzio et al., 2011; Baggini et al., 2014). The ways in which ocean acidification affects communities of primary producers are likely to vary regionally, depending on the species present and abiotic factors such as temperature, light and nutrient availability (Giordano et al., 2005; Brodie et al., 2014; Hofmann et al., 2014).

To begin to understand the influence of physicochemical factors on the responses of macroalgae to ocean acidification, we grew common types of brown algae (from the Families Fucales and Dictyotales) at CO_2 seeps in a multifactorial experiment in which we manipulated light (irradiance) and nutrient levels. At low light levels, macroalgae are thought to be more likely to rely on carbon uptake via diffusion than use energetically expensive carbon concentrating mechanisms (Raven and Beardall, 2014; Raven et al., 2014) which has led to the idea that any benefits of ocean acidification on growth would only be seen at lower light levels for the majority of species (Hepburn et al., 2011). However, ocean acidification also has the potential to damage photoprotective mechanisms which kick-in at high light levels (Pierangelini et al., 2014). Algae minimize damage from high irradiance by down-regulating photosystems-they also produce chemicals, such as phenolic compounds in the brown algae, which screen ultraviolet light and dissipate energy (Figueroa et al., 2014a). In oligotrophic waters, such as those of the Mediterranean, nutrient availability generally limits macroalgal growth (Ferreira et al., 2011), photosynthetic capacity (Pérez-Lloréns et al., 1996) and photoprotective mechanisms (Celis-Plá et al., 2014a).

Our study centers upon a highly oligotrophic region (the Tyrrhenian Sea) which is undergoing rapid changes in carbonate chemistry coupled with coastal eutrophication and increased land run-off (Oviedo et al., 2015). In this region, as with elsewhere in the world, canopy-forming brown algae have undergone a decline in abundance due to anthropogenic perturbation (Scherner et al., 2013; Strain et al., 2014; Yesson et al., 2015). Here, we investigate the interactive effects of increasing CO_2 levels and eutrophication on *Cystoseira compressa* and *Padina pavonica* using a pH gradient caused by volcanic seeps. These species were chosen because they are abundant around shallow Mediterranean CO_2 seeps (Baggini et al., 2014), because *Cystoseira* spp. are indicators of high water quality in the Mediterranean (Bermejo et al., 2013) and since *Padina* spp. tolerate loss of external calcification as CO_2 levels increase (Johnson et al., 2012; Pettit et al., 2015).

Macroalgal responses to ocean acidification may well depend upon their nutrient metabolism, which can vary widely between species (Hofmann et al., 2014; Hurd et al., 2014). Here, we compared interspecific physiological and biochemical responses to ocean acidification under different light and nutrient levels using standard methods for the study of multiple physical stressors in algae (Martínez et al., 2012; Celis-Plá et al., 2014a). Our hypothesis was that both brown algal species would benefit from ocean acidification in shaded conditions when nutrient levels were elevated. We expected that high light levels would inhibit photosystems, and that any benefits from high CO_2 would only occur if sufficient nutrients were available. If this were true we expected to observe increased photosynthetic activity (using electron transport rates and carbon content as a proxy) and increases in phenolic and antioxidant production in shaded nutrient-enriched treatments.

Materials and Methods

Experimental Design

Macroalgal incubations took place from 19 to 22 March 2013, along a CO_2 gradient near Vulcano, Italy (**Figure 1**; Boatta et al., 2013). *Cystoseira compressa* and *Padina pavonica* were collected at 0.5 m depth from a reference zone. Thalli (5 g fresh weight) were held in individual mesh cylinders (15 cm long × 5 cm in diameter) set 1 m apart and suspended at 0.2 m depth off a floating line that was anchored to the seabed perpendicular to the coast. This array was replicated at an ambient CO_2 site (*ca* 500 μatm CO_2), a medium CO_2 site (*ca* 700–800 μatm CO_2) and a high CO_2 site (*ca* 1200 μatm CO_2) (**Table 1**).

Each CO_2 zone had 12 replicates per treatment per species (nutrient enriched + ambient light or 100%$_{PAB}$, i.e., 100% of surface irradiance defined as PAB irradiance (PAR + UVR), nutrient enriched + shaded light or 70%$_{PAB}$, i.e., 70% of surface irradiance defined as PAB irradiance (PAR + UVR), non-enriched + ambient light or 100%$_{PAB}$, non-enriched shaded light

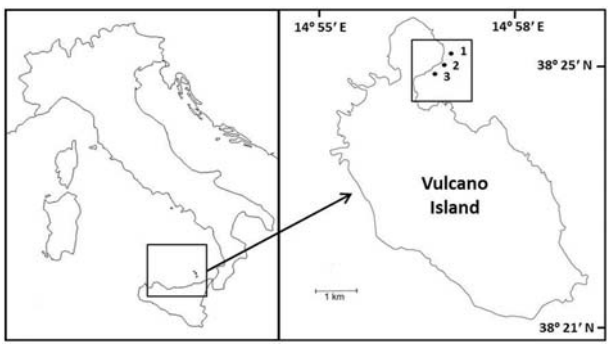

FIGURE 1 | Sample sites and location of experiments on *Cystoseira compressa* and *Padina pavonica* off Vulcano, Italy; (1) Ambient CO_2 site (*ca* 500 μatm CO_2), (2) Medium CO_2 site (*ca* 700–800 μatm CO_2) and (3) High CO_2 (*ca* 1200 μatm CO_2).

TABLE 1 | Seawater carbonate chemistry at three sites off Vulcano Island.

	Ambient CO_2	Medium CO_2	High CO_2
Salinity	38.19 ± 0.03	38.21 ± 0.04	38.23 ± 0.04
Temperature (°C)	14.94 ± 0.21	14.99 ± 0.13	15.06 ± 0.19
pH_{NBS}	8.11 ± 0.02	7.97 ± 0.04	7.86 ± 0.09
pCO_2 (μatm)	512 ± 29	779 ± 109	1250 ± 410
CO_2 (μmol kg^{-1})	18.8 ± 1.2	28.7 ± 4.1	46 ± 15.3
HCO_3^- (μmol kg^{-1})	2129 ± 20	2161 ± 23	2236 ± 36
CO_3^{2-} (μmol kg^{-1})	181 ± 8.3	138 ± 9.3	119 ± 14.6
Total Alkalinity (μmol kg^{-1})	2527 ± 46	2499 ± 14	2569 ± 427
Ω Calcite	4.21 ± 0.19	3.22 ± 0.22	2.78 ± 0.34
Ω Aragonite	2.71 ± 0.13	2.07 ± 0.14	1.79 ± 0.22

Island, with an ambient CO_2, a Medium CO_2 and a High CO_2 site. Temperature (°C), Salinity and pH (NBS scale) were collected on different days in March 2013 (mean values ± SE, n = 5 – 14). Average total alkalinity (μmol kg^{-1}) was calculated from water samples collected at each site on 20th March 2013 (mean values ± SE, n = 3).

or 70%$_{PAB}$). Light levels were manipulated using a 1 mm^2 size pore mesh that reduced light levels to 70% of that of the unshaded treatments. The filter we used does not modify the light spectra (Aphalo et al., 2013). Mesh bags containing 100 g of a slow-release fertilizer comprising 17% N (NH_4^+ and NO_3^-), 17% P (P_2O_5) and 17% K (Multicote®, Haifa Chemicals, USA) were attached below nutrient enriched cylinders. For the non-enriched treatments, a bag with 100 g of sand was used as a control. The nutrient treatments were set 20 m apart from each other so that non-enriched treatments were unaffected.

Environmental Conditions

The seawater carbonate system was monitored at each site (**Table 1**). A 556 MPS YSI (Yellow Springs, USA) probe was used to measure salinity, pH and temperature (°C). The pH sensor was calibrated using NBS scale standard buffers. On 20th March 2013, water samples for total alkalinity (TA) were strained through 0.2 μm filters, poisoned with 0.05 ml of 50% $HgCl_2$, and then stored in the dark at 4°C. Three replicates were analyzed at 25°C using a titrator (Mettler Toledo, Inc.). The pH was measured at 0.02 ml increments of 0.1 N HCl.

Total alkalinity was calculated from the Gran function applied to pH variations from 4.2 to 3.0, from the slope of the curve HCl volume vs. pH. The pCO_2 and the saturation state of aragonite were calculated from pH_{NBS}, TA, temperature and salinity using the CO_2 SYS package (Pierrot and Wallace, 2006), using the constants of Roy et al. (1993) and Dickson (1990). Saturation state (Ω) is the ion product of calcium and carbonate ion concentrations as:

$$\Omega = [Ca^{2+}][CO_3^{2-}]/K'sp \quad (1)$$

The apparent solubility product K'sp depends on temperature, salinity, pressure, and the particular mineral phase (e.g. calcite and aragonite in this case).

Irradiance was monitored at the sea surface at two wavelength bands using PAR (QSO-SUN 2.5V) and UV-A (USB-SU 100, Onset Computer Corporation, Massachusetts, USA) sensors sealed in a water proof box (OtterBox3000). Water temperature was monitored using a HOBO logger (Onset Computer Corporation, Massachusetts, USA). The nutrient enrichment caused by the release of the fertilizer was assessed taking triplicate seawater samples at both enriched and non-enriched sites. Seawater was strained using portable GF/F filters (Whatman International. Ltd., Maidstone, UK) then transported to the laboratory inside an isotherm bag (4°C, in darkness), and kept at −20°C. Nitrate (NO_3^-) was determined using an automated analyzer (SanPlus^{++} System, SKALAR, Breda, Netherlands) applying standard colorimetric procedures (Koroleff, 1983).

Physiological and Biochemical Variables

Several physiological variables were obtained from the algae within each cylinder at the end of the experiment. These variables were also measured in *C. compressa* and *P. pavonica* from ambient CO_2 site (500 μatm) populations at 0.5 m depth. Carbon and nitrogen contents were determined using an element analyzer CNHS-932 model (LECO Corporation, Michigan, USA).

In vivo chlorophyll *a* fluorescence associated with Photosystem II was determined by using a portable pulse amplitude modulated (PAM) fluorometer (Diving-PAM, Walz GmbH, Germany). Macroalgal thalli were collected from natural populations (initial time) and after 4 days of incubation in the experiment (for each treatment or cylinder), and were put in 10 mL incubation chambers to obtain rapid light curves for each treatment. F_o and F_m were measured after 15 min in darkness to obtain the maximum quantum yield (F_v/F_m) being $F_v = F_m – F_o$, F_o the basal fluorescence of 15 min dark adapted thalli and F_m maximal fluorescence after a saturation light pulse of >4000 μmol m^{-2} s^{-1} (Schreiber et al., 1995). The electron transport rate (ETR) was determined after 20 s exposure in eight increasing irradiances of white light (halogen lamp provided by the Diving-PAM). The ETR was calculated according to Schreiber et al. (1995) as follows:

$$ETR\ (\mu mol\ electrons\ m^{-2}s^{-1}) = \Delta F/F'_m \times E \times A \times F_{II} \quad (2)$$

where $\Delta F/F'_m$ is the effective quantum yield, being $\Delta F = Fm' - Ft$ (Ft is the intrinsic fluorescence of alga incubated in light and Fm' is the maximal fluorescence reached after a saturation pulse of algae incubated in light), E is the incident PAR irradiance expressed in μmol photons m^{-2} s^{-1}, A is the thallus absorptance as the fraction of incident irradiance that is absorbed by the algae (see Figueroa et al., 2003) and F_{II} is the fraction of chlorophyll related to PSII (400–700 nm) being 0.8 in brown macroalgae (Figueroa et al., 2014a). ETR parameters as maximum electron transport rate (ETR_{max}) and the initial slope of ETR vs. irradiance function (α_{ETR}) as estimator of photosynthetic efficiency were obtained from the tangential function reported by Eilers and Peeters (1988). Finally, the saturation irradiance for ETR (Ek_{ETR}) was calculated from the intercept between ETR_{max} and α_{ETR}. Non-photochemical quenching (NPQ) was calculated according to Schreiber et al. (1995) as:

$$NPQ = (F_m - F'_m)/F'_m \quad (3)$$

Maximal NPQ (NPQ_{max}) and the initial slope of NPQ vs. irradiance function (α_{NPQ}) were obtained from the tangential

function of NPQ vs. irradiance function according to Eilers and Peeters (1988).

Pigments were extracted from 20 mg fresh weight of thalli using 2 mL of 100% acetone and analyzed using an ultra-high-performance liquid chromatographer (Shimadzu Corp., Kyoto, Japan) equipped with a photodiode array detector to measure peaks in the range 350–800 nm. After extraction samples were centrifuged at 16200 g for 5 min (Sorvall Legend Micro 17, Thermo Scientific, Langenselbold, Germany) and then the extracts were filtered (0.22 μm nylon filters). The separation, was achieved with one column C-18 reversed phase (Shim-pack XR-ODS column; 3.0 × 75 mm i. d.; 2.2 μm particle size; Shimadzu, Kyoto, Japan) protected by a guard column TR-C-160 K1 (Teknokroma, Barcelona, Spain). The carotenoid composition was determined according to García-Plazaola and Becerril (1999) with some modifications (García-Plazaola et al., 2012), using commercial standards (DHI LAB Products). The mobile phase consisted of two components: Solvent A, acetonitrile: methanol: Tris buffer (0.1 M, pH 8) (84:2:14); and solvent B, methanol: ethyl acetate (68:32). The pigments were eluted using a linear gradient from 100% A to 100% B for the first 7 min, followed by an isocratic elution with 100% B for the next 4 min. This was followed by a 50 s linear gradient from 100% B to 100% A and an isocratic elution with 100% B for the next 3 min to allow the column to re-equilibrate with solvent A, prior to the next injection.

Total phenolic compounds were determined using 0.25 g fresh weight samples pulverized with a mortar and pestle with sand and 2.5 mL of 80% methanol. After keeping the samples overnight at 4°C, the mixture was centrifuged at 2253 g for 30 min at 4°C, and then the supernatant was collected. Total phenolic compounds were determined colorimetrically using Folin-Ciocalteu reagent and phloroglucinol (1,3,5-trihydroxybenzene, Sigma P-3502) as standard. Finally the absorbance was determined at 760 nm using a spectrophotometer (UV Mini-1240, Shimadzu) (Celis-Plá et al., 2014b). Total phenolic content was expressed as mg g^{-1} DW after determining the fresh to dry weight ratio in the tissue (5.2 for *C. compressa* and 4.5 *P. pavonica*, respectively). The results are expressed as average ± SE from three replicates of each treatment. Antioxidant activity was measured on polyphenol extracts according to Blois (1958); 150 μL of DPPH (2,2-diphenyl-1-picrylhydrazyil) prepared in 90% methanol were added to each extract. The reaction was complete after 30 min in darkness at ambient temperature (∼20°), and the absorbance was read at 517 nm in a spectrophotometer (UVmini-1240, Shimadzu). The calibration curve made from DPPH was used to calculate the remaining concentration of DPPH in the reaction mixture after incubation. Values of DPPH concentration (mM) were plotted against plant extract concentration expressed as the EC_{50} value (oxidation index, mg DW mL^{-1}) required to scavenge 50% of the DPPH in the reaction mixture. Ascorbic acid was used as a control (Celis-Plá et al., 2014b).

Statistical Analysis

The effects of the *in situ* treatments on the physiological responses of *C. compressa* and *P. pavonica* were assessed using analysis of variance. Three fixed factors were considered: Site with three levels: ambient CO_2 site, medium CO_2 and high CO_2, Irradiance with two levels: 70 and 100% of surface irradiance (PAR + UVR irradiance), and two nutrient levels; enriched (N+) and non-enriched (N). This design allowed us to test interactive and additive effects of the variables on physiological responses after the 4 day experimental period. Student Newman Keuls tests (SNK) were performed on significant ANOVA interactions. Homogeneity of variance was tested using Cochran tests and by visual inspection of the residuals. All data conformed to homogeneity of variance. Analyses were performed by using SPSS v.21 (IBM, USA).

Results

Environmental Conditions

Cystoseira compressa and *Padina pavonica* were abundant at all three stations; *P. pavonica* was visibly less calcified at the site with the highest levels of CO_2. The seawater temperature was about15°C and the salinity was 38 at all stations; at the Ambient site, mean pH was 8.11, at the Medium CO_2 site (700–800 μatm), mean pH was 7.97 and at the High CO_2 site (1200 μatm), it was 7.86 (**Table 1**).

The average daily irradiance for the experimental period was 5360 kJ m^{-2} for PAR and 666 kJ m^{-2} for UVA. The nutrient enriched treatments had approximately 100 times the nitrate concentration of the ambient seawater; ambient vs. enriched ratios were 0.16 ± 0.04 vs. 106.17 ± 9.37 μM for the ambient site, 0.13 ± 0.01 vs. 106.33 ± 9.37 μM at the medium CO_2 site and 0.25 μM ± 0.01 vs. 106.42 ± 9.37 μM at the high CO_2 site (mean ± SE, $n = 3$).

Physiological and Biochemical Responses

The carbon content of *C. compressa* increased with increasing CO_2, whereas in *P. pavonica* showed interactive effects between all factors. Carbon, in *P. pavonica* showed maximal values 279.9 ± 6.5 with increased CO_2, in non-enrichment enriched treatments and minimal values 225.3 ± 2.4 mg g^{-1} DW with decreased CO_2, non-nutrient enriched and 70%$_{PAB}$ conditions (**Table 2**, Table S1). The nitrogen content of *C. compressa* was greatest in the high CO_2, nutrient enriched and 70%$_{PAB}$ treatment (**Figure 2A**, Figure S1); conversely, in *P. pavonica* the nitrogen content was highest at the reference site, ambient CO_2 treatment (**Figure 2B**, Figure S1). The ratio C:N of *C. compressa* did not show significant differences between treatments (**Figure 3A**, Figure S1), whereas the ratio in *P. pavonica* showed significant effects for CO_2 levels and nutrient enrichment showed maximal values (19.5 ± 5.8) with increased CO_2, non-nutrient enriched in 100%$_{PAB}$ conditions and minimal values 15.9 ± 0.5 in medium CO_2, nutrient enrichment and 70%$_{PAB}$ conditions (**Figure 3B**, Figure S1).

The maximal quantum yield (F_v/F_m) was significantly different between CO_2 treatments, nutrient and irradiance in both macroalgae (**Figure 4**, Figure S2). In *C. compressa*, the F_v/F_m was greatest in 70%$_{PAB}$ treatments with high CO_2, and non-enriched enrichment (**Figure 4A**, Figure S2), but in *P. pavonica*

TABLE 2 | Carbon content, photosynthetic efficiency (α_{ETR}), maximal electron transport rate (ETR_{max}), expressed in μmol m^{-2} s^{-1}), irradiance of saturation of ETR (Ek_{ETR}), maximal non-photochemical quenching (NPQ_{max}) (mean values ± SE, $n = 3$) of *Cystoseira compressa* and *Padina pavonica* in relation to Irradiance (70%$_{PAB}$: low irradiance and 100%$_{PAB}$: ambient irradiance), Nutrients (Nutrient+ and Ambient Nutrient) and CO_2 (ambient CO_2 site: 500 μatm, Medium CO_2 site: 700–800 μatm and High CO_2: 1200 μatm) treatments.

		Cystoseira compressa					*Padina pavonica*				
		It	**Nutrient+**		**Ambient nutrient**		***It***	**Nutrient+**		**Ambient nutrient**	
			70%$_{PAB}$	***100%$_{PAB}$***	***70%$_{PAB}$***	***100%$_{PAB}$***		***70%$_{PAB}$***	***100%$_{PAB}$***	***70%$_{PAB}$***	***100%$_{PAB}$***
Carbon	*Ambient CO_2*	264.3 ± 8.4	266.3 ± 5.1	271.4 ± 2.7	261.7 ± 5.5	266.3 ± 7.6	274.0 ± 13.7	276.9 ± 5.9^{c}	254.8 ± 3.3^{bc}	225.3 ± 2.4^{a}	263.7 ± 0.8^{bc}
	Medium CO_2		253.2 ± 11.4	251.7 ± 3.4	252.2 ± 1.9	261.9 ± 5.2		240.0 ± 5.6^{ab}	243.0 ± 9.4^{ab}	226.8 ± 7.2^{a}	256.4 ± 7.4^{bc}
	High CO_2		276.2 ± 2.7	259.6 ± 8.6	273.2 ± 6.6	273.2 ± 6.6		271.1 ± 4.3^{c}	257.5 ± 4.4^{bc}	279.9 ± 6.5^{c}	275.7 ± 2.3^{c}
α_{ETR}	*Ambient CO_2*	0.31 ± 0.02	0.39 ± 0.02^{bc}	0.25 ± 0.06^{ab}	0.32 ± 0.07^{abc}	0.34 ± 0.01^{abc}	0.34 ± 0.01	0.28 ± 0.01^{b}	0.15 ± 0.02^{ab}	0.09 ± 0.02^{a}	0.27 ± 0.05^{b}
	Medium CO_2		0.32 ± 0.02^{abc}	0.34 ± 0.01^{abc}	0.20 ± 0.03^{a}	0.33 ± 0.01^{abc}		0.25 ± 0.02^{b}	0.23 ± 0.03^{b}	0.15 ± 0.03^{ab}	0.24 ± 0.03^{b}
	High CO_2		0.21 ± 0.02^{a}	0.40 ± 0.02^{bc}	0.43 ± 0.01^{c}	0.24 ± 0.03^{ab}		0.28 ± 0.02^{b}	0.19 ± 0.02^{ab}	0.23 ± 0.02^{b}	0.24 ± 0.02^{b}
ETRmax	*Ambient CO_2*	46.8 ± 5.3	55.5 ± 15.3^{a}	65.2 ± 13.1^{abc}	85.1 ± 9.2^{bc}	112.4 ± 12.9^{c}	51.8 ± 2.0	41.7 ± 1.7	49.0 ± 1.5	49.6 ± 3.8	57.9 ± 7.5
	Medium CO_2		60.1 ± 13.4^{abc}	86.2 ± 2.0^{bc}	67.0 ± 9.8^{abc}	73.8 ± 11.7^{abc}		42.4 ± 6.3	60.2 ± 6.9	48.6 ± 9.5	57.1 ± 3.7
	High CO_2		32.5 ± 7.9^{a}	101.1 ± 7.9^{bc}	95.1 ± 12.0^{bc}	63.7 ± 8.1^{abc}		42.5 ± 2.9	59.0 ± 3.8	64.4 ± 12.3	73.4 ± 5.5
Ek_{ETR}	*Ambient CO_2*	152.7 ± 6.8	139.9 ± 35.1	261.8 ± 33.8	281.5 ± 40.6	324.2 ± 31.3	150.1 ± 4.0	149.3 ± 8.3^{a}	339.5 ± 34.5^{cd}	416.7 ± 11.6^{d}	218.7 ± 17.9^{abc}
	Medium CO_2		187.1 ± 32.5	252.9 ± 5.0	337.6 ± 7.0	227.1 ± 42.8		174.9 ± 25.6^{ab}	262.2 ± 17.8^{abc}	329.9 ± 32.4^{cd}	319.7 ± 71.0^{bcd}
	High CO_2		154.1 ± 15.9	255.1 ± 33.1	221.9 ± 30.2	278.5 ± 62.7		156.1 ± 25.3^{a}	323.2 ± 29.9^{bcd}	224.8 ± 40.7^{abc}	313.6 ± 31.9^{bcd}
NPQmax	*Ambient CO_2*	1.61 ± 0.33	2.14 ± 0.58^{b}	0.48 ± 0.04^{a}	0.62 ± 0.02^{a}	3.24 ± 0.31^{c}	1.95 ± 0.39	1.91 ± 0.36^{bc}	0.31 ± 0.09^{a}	0.12 ± 0.02^{a}	1.97 ± 0.33^{bc}
	Medium CO_2		3.65 ± 0.33^{c}	1.40 ± 0.15^{ab}	0.47 ± 0.20^{a}	0.57 ± 0.10^{a}		3.32 ± 0.44^{d}	1.28 ± 0.33^{abc}	0.70 ± 0.13^{ab}	0.72 ± 0.01^{ab}
	High CO_2		2.21 ± 0.29^{b}	3.69 ± 0.19^{c}	1.84 ± 0.22^{b}	0.59 ± 0.17^{a}		2.39 ± 0.31^{c}	0.91 ± 0.18^{ab}	1.46 ± 0.52^{abc}	0.68 ± 0.13^{ab}

It: Initial time of the experimental period is shown in the first column. Lower-case letters denote significant differences after SNK test.

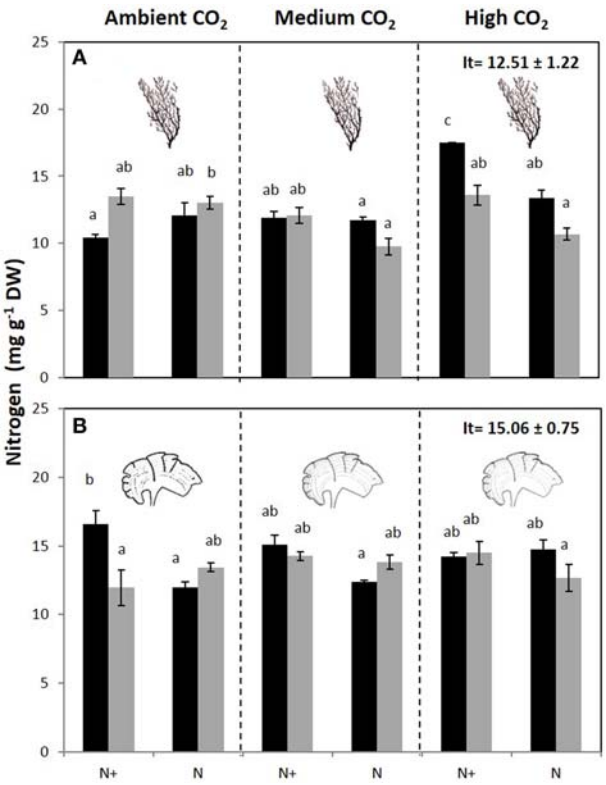

FIGURE 2 | Nitrogen content (mg g^{-1} DW) (mean ± SE, $n = 3$) in (A) *Cystoseira compressa* and (B) *Padina pavonica* at Ambient CO_2 (*ca* 500 μatm, left boxes), Medium CO_2 (*ca* 700–800 μatm, middle boxes) and High CO_2 (*ca* 1200 μatm, right boxes), in Irradiance and Nutrient treatments. Dark bars indicate 70%$_{PAB}$ (low irradiance), gray bars indicate 100%$_{PAB}$ (ambient irradiance). N+ and N indicate nutrient enriched and non-enriched treatments respectively. Upper values in right box indicate initial time values (It: mean ± SE, $n = 3$). Lower-case letters denote significant differences after an SNK test.

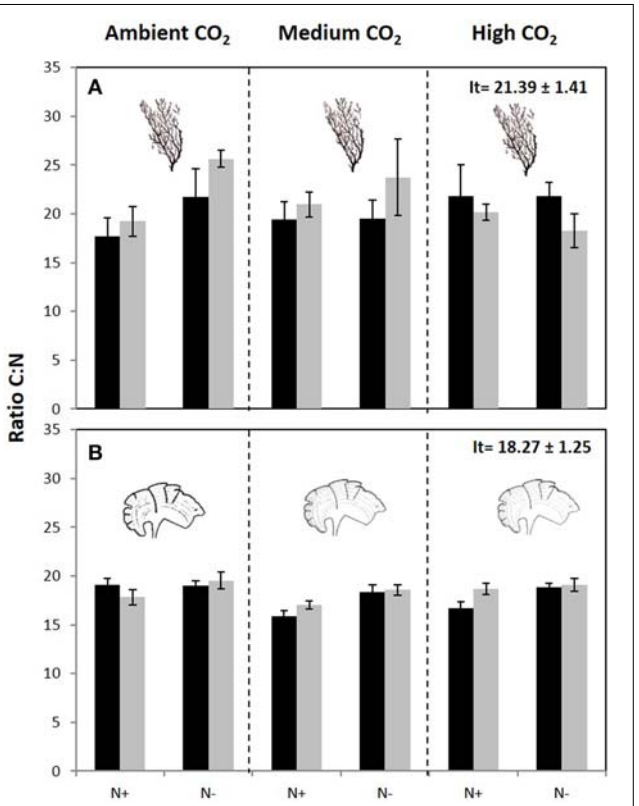

FIGURE 3 | C:N ratio (mean ± SE, $n = 3$) in (A) *Cystoseira compressa* and (B) *Padina pavonica* at Ambient CO_2 (*ca* 500 μatm, left boxes), Medium CO_2 (*ca* 700–800 μatm, middle boxes) and High CO_2 (*ca* 1200 μatm, right boxes), in Irradiance and Nutrient treatments. Dark bars indicate 70%$_{PAB}$ (low irradiance), gray bars indicate 100%$_{PAB}$ (ambient irradiance). N+ and N indicate nutrient enriched and non-enriched treatments respectively. Upper values in right box indicate initial time values (It: mean ± SE, $n = 3$).

this was greatest in the nutrient enriched treatments (**Figure 4B**, Figure S2). The α_{ETR} values also varied significantly between treatments in both species (**Table 2**, Table S2). In *C. compressa,* α_{ETR} was greatest in 70%$_{PAB}$ treatments at high CO_2 with non-enriched enrichment; in *P. pavonica* α_{ETR} was greatest in the high CO_2 conditions (**Table 2**, Table S2). ETR_{max} in *C. compressa* was highest in high CO_2, 70%$_{PAB}$ and non-nutrient enrichment, also in 100%$_{PAB}$ and nutrient enrichment, and also this was higher with decreased CO_2, 100%$_{PAB}$, in non-nutrient enrichment. In *P. pavonica*, ETR_{max} varied significantly depending on nutrient and irradiance, without interactions (**Table 2**, Table S2). In contrast, the Ek_{ETR} in *C. compressa* had one significant interaction among nutrient x irradiance. *P. pavonica* had significant interactions between CO_2 level, nutrient and irradiance. The Ek_{ETR}, in *C. compressa*, was greatest in the 100%$_{PAB}$ treatments that had no CO_2 or nutrient enrichment, but in *P. pavonica* Ek_{ETR} was greatest in 70%$_{PAB}$ conditions (**Table 2**, Table S2). In both species, the maximal non-photochemical quenching (NPQ_{max}) was affected by the interaction of all factors. In *C. compressa*, NPQ_{max} increased significantly with increasing CO_2 conditions, under nutrient enriched and 100%$_{PAB}$, also increased in *ca* 700–800 μatm but in 70%$_{PAB}$. As well as, NPQ_{max} increased under ambient CO_2 conditions in 100%$_{PAB}$ in nutrient non-enriched. Finally, in *P. pavonica,* the NPQ_{max} was significantly higher in 70%$_{PAB}$ at 700 μatm CO_2 treatment with nutrient enrichment (**Table 2**, Table S2).

Nutrient enrichment increased Chl*a* significantly in *C. compressa*. In contrast, in *P. pavonica* significant differences were found for the following interactions: CO_2 level × nutrient, CO_2 level × irradiance and nutrient × irradiance (**Table 3**, Table S3). The same occurred for Chl*c* in *P. pavonica*; but there was no significant difference in *C. compressa* (**Table 3**, Table S3). The carotenoids, fucoxanthin and violaxanthin in *C. compressa* did not differ among factors (**Table 3**, Table S3) but in *P. pavonica* the fucoxanthin and violaxanthin contents were affected by the interaction of all factors. Fucoxanthin increased in 70%$_{PAB}$, non-enriched treatments in ambient CO_2 whereas violoxanthin levels were highest in 70%$_{PAB}$, *ca* 700–800 μatm CO_2, nutrient enriched treatment (**Table 3**, Table S3).

Phenolic content (PC) was affected by the interaction of all factors in both species (**Figure 5**, Figure S4). In *C. compressa*, PC

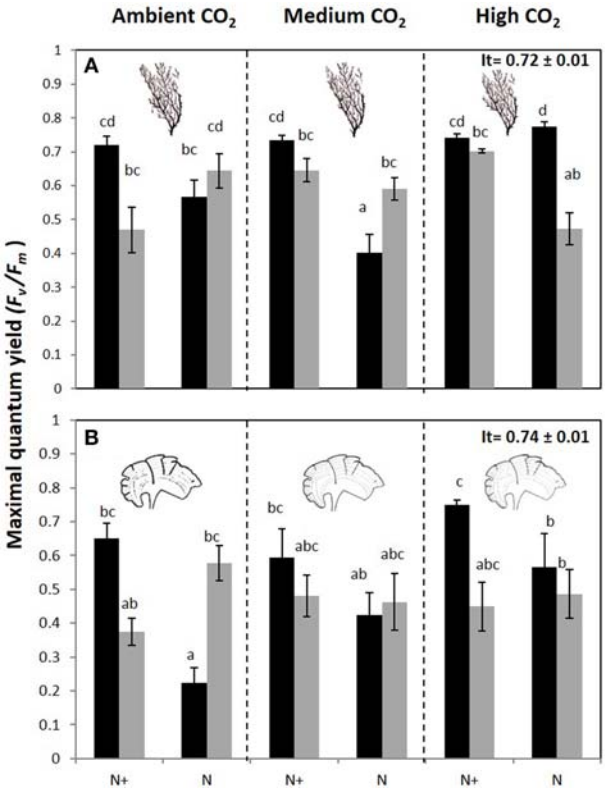

FIGURE 4 | Maximal quantum yield or F_v/F_m (mean ± SE, $n = 3$) in (A) *Cystoseira compressa* and (B) *Padina pavonica* at Ambient CO_2 (*ca* 500 μatm, left boxes), Medium CO_2 (*ca* 700–800 μatm, middle boxes) and High CO_2 (*ca* 1200 μatm, right boxes), in Irradiance and Nutrient treatments. Dark bars indicate $70\%_{PAB}$ (low irradiance), and gray bars indicate $100\%_{PAB}$ (ambient irradiance). N+ and N indicate nutrient enriched and non-enriched treatments respectively. Upper values in right box indicate initial time values (It: mean ± SE, $n = 3$). Lower-case letters denote significant differences after an SNK test.

was highest in CO_2 and nutrient enriched conditions (**Figure 5A**, Figure S4). In *P. pavonica* at 1200 μatm CO_2, PC was high in $100\%_{PAB}$ and nutrient enriched treatments and in $70\%_{PAB}$ treatments non-nutrient enrichment (**Figure 5B**, Figure S4). Antioxidant activity (EC_{50}) showed a significant interaction between CO_2 level × nutrient and CO_2 level × irradiance in *C. compressa*; however in *P. pavonica* the only significant difference found in antioxidant activity was between CO_2 level and irradiance. In *C. compressa* and *P. pavonica*, EC_{50} was lowest (i.e., it had higher antioxidant activity) in the high CO_2, $70\%_{PAB}$ light conditions and nutrient enriched treatments (**Table 3**, Table S4).

Discussion

Recent reviews surmise that ocean acidification is likely to increase macroalgal productivity due to beneficial effects of increased dissolved inorganic carbon (DIC) levels which can stimulate the growth of algae and allows them to divert more resources into anti-herbivore and photo-protective compounds (Harley et al., 2012; Brodie et al., 2014). Here we show that calcified and non-calcified macroalgae can indeed benefit physiologically from increases in DIC, but that the benefits, and the extent of the algal response, depend upon nutrient and light availability. **Figure 6** summarizes our projections that brown macroalgal stands will both proliferate in the shallows (because of up-regulation of anti-herbivore and photo-protective compounds) and extend deeper due to a combination of ocean acidification and anthropogenic nutrient input, whereas other work on Mediterranean CO_2 seeps has established that sea urchins and coralline algae are adversely affected by acidification (Baggini et al., 2014). *In vivo* chlorophyll *a* fluorescence parameters (maximal quantum yield or F_v/F_m and maximal electron transport rate or ETR_{max}) and algal biochemical composition (Chl*a*, total phenolic compounds and antioxidant activity, %C) helps explain the dominance of phaeophytes at a variety of coastal Mediterranean CO_2 seeps. Increases in brown macroalgal cover at CO_2 seep sites are probably due to a combination of the direct stimulus of increased DIC for photosynthesis for species with inefficient carbon concentrating mechanisms (CCMs), and decreased grazing since sea urchins for example are excluded by hypercapnia (Calosi et al., 2013).

Other Mediterranean seep locations show similar trends to Vulcano, with increases in *Cystoseira* and *Padina* species at elevated CO_2 locations compared to reference locations (Johnson et al., 2012; Baggini et al., 2014). Work in other regions has also shown that ocean acidification can directly benefit some macroalgae, such as *Gracilaria lemaneiformis* in China (Zou and Gao, 2009) and mat-forming *Feldmannia* spp. in Australia (Russell et al., 2011), as well as canopy-forming phaeophytes such as *Nereocystis luetkeana* and *Macrocystis pyrifera* (Swanson and Fox, 2007; Roleda et al., 2012). We found that the benefits of increased DIC were even more pronounced when combined with increased nutrients. This is what we expected, given that macroalgae tend to be nutrient-limited in oligotrophic waters such as those of the Mediterranean Sea (Ferreira et al., 2011). Both our study species increased electron transport rates and the accumulation of photoprotectors when exposed to a Nitrogen Phosphorus Potassium fertilizer, but these were short-term experiments with macroalgae grown in isolation. We suspect that chronic eutrophication combined with ocean acidification may benefit more opportunistic algal groups, to the detriment of brown macroalgae based on research by Russell et al. (2009) and Falkenberg et al. (2013). In our study, *C. compressa* and *P. pavonica* had increased carbon content at elevated CO_2, which was augmented by increases in a range of other physiological parameters when nutrient levels were also increased. The F_v/F_m ratio was highest at increased CO_2 concentrations with no nutrient enrichment in *C. compressa*, but highest at increased CO_2 with nutrient enrichment for *P. pavonica* (**Figure 4**). The maximal photosynthetic activity (ETR_{max}) in *C. compressa* was reduced at high nutrient levels in shaded conditions but in fully lit conditions nutrients did not have significant effects under high DIC conditions. In other *Cystoseira* species, such as *C. tamariscifolia*, both F_v/F_m and ETR_{max} also decrease in nutrient enriched treatments in field experiments at various

TABLE 3 | Pigment contents; Chlorophyll *a* (Chl*a*), chlorophyll *c* (Chl*c*), Fuxocanthin and Violaxanthin contents are expressed in mg g^{-1} DW and Antioxidant activity expressed as EC_{50} in mg DW mL^{-1} (mean values ± SE, $n = 3$) of *Cystoseira compressa* and *Padina pavonica* in relation to Irradiance (70%$_{PAB}$: low irradiance and 100%$_{PAB}$: ambient irradiance), Nutrient (Nutrient+ and Ambient Nutrient) and CO_2 (ambient CO_2 site: 500 μatm, Medium CO_2 site:700-800 μatm and High CO_2: 1200 μatm) treatments.

		Cystoseira compressa					*Padina pavonica*				
		It	**Nutrient+**		**Ambient nutrient**		***It***	**Nutrient+**		**Ambient nutrient**	
			70%$_{PAB}$	***100%$_{PAB}$***	***70%$_{PAB}$***	***100%$_{PAB}$***		***70%$_{PAB}$***	***100%$_{PAB}$***	***70%$_{PAB}$***	***100%$_{PAB}$***
Chla	*Ambient CO_2*	1.19 ± 0.17	1.41 ± 0.21	1.29 ± 0.27	0.86 ± 0.16	0.86 ± 0.36	0.80 ± 0.08	0.78 ± 0.05	0.70 ± 0.04	0.23 ± 0.03	0.67 ± 0.01
	Medium CO_2		1.61 ± 0.13	1.32 ± 0.11	1.09 ± 0.25	1.34 ± 0.28		0.95 ± 0.11	0.41 ± 0.08	0.57 ± 0.10	0.69 ± 0.02
	High CO_2		1.67 ± 0.18	1.65 ± 0.47	1.06 ± 0.25	1.42 ± 0.41		0.77 ± 0.40	0.32 ± 0.08	0.75 ± 0.03	0.75 ± 0.08
Chlc	*Ambient CO_2*	0.19 ± 0.09	0.45 ± 0.22	0.61 ± 0.23	0.52 ± 0.22	0.21 ± 0.07	0.86 ± 0.15	0.04 ± 0.02	0.09 ± 0.03	0.35 ± 0.10	0.04 ± 0.01
	Medium CO_2		0.08 ± 0.01	0.15 ± 0.06	0.04 ± 0.01	0.07 ± 0.01		0.09 ± 0.02	0.07 ± 0.01	0.35 ± 0.08	0.11 ± 0.06
	High CO_2		0.11 ± 0.04	0.52 ± 0.22	0.49 ± 0.27	0.39 ± 0.16		0.08 ± 0.01	0.46 ± 0.02	0.08 ± 0.01	0.08 ± 0.06
Fucoxanthin	*Ambient CO_2*	2.91 ± 0.13	0.44 ± 0.10	0.40 ± 0.12	0.38 ± 0.02	0.39 ± 0.05	0.83 ± 0.09	0.19 ± 0.04^{a}	0.26 ± 0.01^{ab}	1.32 ± 0.06^{c}	0.20 ± 0.04^{a}
	Medium CO_2		0.55 ± 0.12	0.47 ± 0.02	0.49 ± 0.13	0.52 ± 0.06		0.46 ± 0.10^{b}	0.18 ± 0.06^{a}	0.36 ± 0.06^{ab}	0.22 ± 0.01^{ab}
	High CO_2		0.66 ± 0.02	0.46 ± 0.04	0.39 ± 0.13	0.55 ± 0.21		0.27 ± 0.08^{ab}	0.29 ± 0.01^{ab}	0.28 ± 0.01^{ab}	0.26 ± 0.02^{ab}
Violaxanthin	*Ambient CO_2*	0.08 ± 0.01	0.07 ± 0.01	0.06 ± 0.02	0.06 ± 0.01	0.06 ± 0.01	0.16 ± 0.01	0.05 ± 0.01^{a}	0.05 ± 0.01^{a}	0.05 ± 0.02^{a}	0.05 ± 0.01^{a}
	Medium CO_2		0.08 ± 0.02	0.07 ± 0.01	0.12 ± 0.02	0.08 ± 0.01		0.15 ± 0.01^{b}	0.03 ± 0.01^{a}	0.06 ± 0.02^{a}	0.04 ± 0.01^{a}
	High CO_2		0.11 ± 0.01	0.07 ± 0.01	0.07 ± 0.01	0.08 ± 0.03		0.05 ± 0.01^{a}	0.06 ± 0.01^{a}	0.06 ± 0.01^{a}	0.02 ± 0.01^{a}
EC_{50}	*Ambient CO_2*	0.56 ± 0.02	0.93 ± 0.11	0.75 ± 0.07	0.94 ± 0.13	0.71 ± 0.06	0.75 ± 0.10	0.86 ± 0.13	0.84 ± 0.19	1.27 ± 0.14	1.00 ± 0.02
	Medium CO_2		0.89 ± 0.01	0.84 ± 0.07	0.73 ± 0.07	0.89 ± 0.09		0.80 ± 0.09	0.92 ± 0.18	0.64 ± 0.09	1.24 ± 0.06
	High CO_2		0.53 ± 0.09	0.77 ± 0.02	0.77 ± 0.09	1.19 ± 0.19		0.71 ± 0.15	0.82 ± 0.10	1.00 ± 0.13	0.87 ± 0.03

It: Initial time of the experimental period is shown in the first column. Lower-case letters denote significant differences after SNK test.

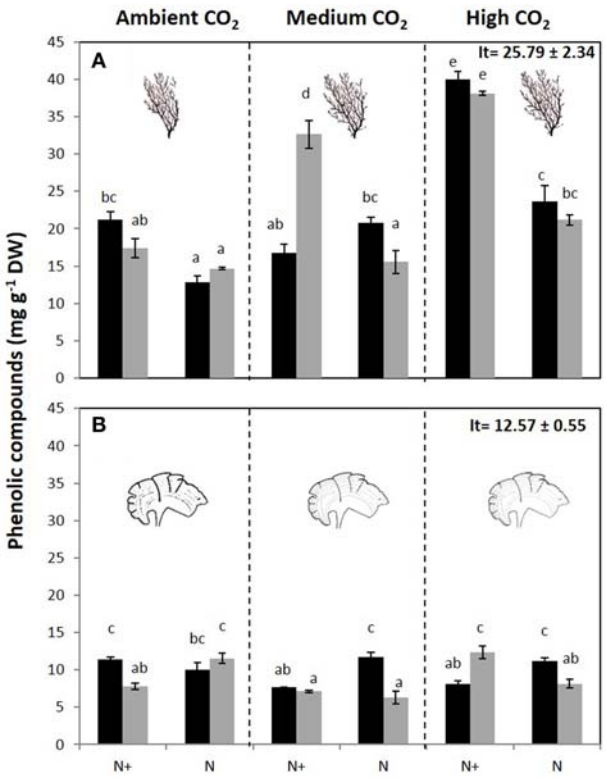

FIGURE 5 | Total phenolic compounds (mg g^{-1} DW) (mean ± SE, $n = 3$) in (A) *Cystoseira compressa* and (B) *Padina pavonica* from Ambient CO_2 (*ca* 500 μatm, left boxes), Medium CO_2 (*ca* 700–800 μatm, middle boxes) and High CO_2 (*ca* 1200 μatm, right boxes), in Irradiance and Nutrient treatments. Dark bars indicate 70%$_{PAB}$ (low irradiance), gray bars indicate 100%$_{PAB}$ (ambient irradiance). N+ and N indicate nutrient enriched and non-enriched treatments respectively. Upper values in right box indicate initial time values (It: mean ± SE, $n = 3$). Lower-case letters denote significant differences after an SNK test.

depths (Celis-Plá et al., 2014a). In another experiment, Celis-Plá et al. (2014b) found the highest ETR_{max} in *C. tamariscifolia* in thalli with the lowest internal nitrogen stores i.e., winter compared to summer grown algae. On the other hand, Ek_{NPQ} increased in all cases with the increased CO_2 as an acclimation to high light levels. On this basis, it is clear that the responses of coastal macroalgal communities to ocean acidification will depend on nutrient availability, and will be species-specific. Given these results we expect that in temperate waters, brown algae will benefit from increases in CO_2 if sufficient nutrients are available (Johnson et al., 2012). However, as with all ecology, we can expect that there will be a region-specific balancing act. We show here that in oligotrophic conditions brown macroalgae were unable to take full advantage of increased inorganic carbon availability. There is added complexity when we consider that many regions have experienced a die-back of canopy-forming brown algae due to excess nutrients or sedimentation (Strain et al., 2014); ocean acidification may exacerbate this problem since increased DIC may further benefit those algae that presently compete with fucoids and kelps in eutrophic conditions (Connell et al., 2013).

Light quantity and quality drive physiological processes in macroalgae (Hanelt and López-Figueroa, 2012), so we were not surprised to find that shading affected their responses to ocean acidification. We anticipated two outcomes of the effects of light: we expected ETR rates to be higher as the most obvious response to light, but we also expected low-light macroalgae to increase ETR rates and %C when transplanted to higher CO_2 concentrations. Our first expectations were met, as maximum quantum yield, photosynthetic efficiency, irradiance of saturation and non-photochemical quenching for chlorophyll fluorescence all increased at higher light levels and were, at times, amplified by increasing CO_2 and nutrient levels. The only instance where our second expectation was met was for *P. pavonica* under ambient nutrients, which had significantly higher %C (and non-significantly higher ETR_{max}) when transplanted to elevated CO_2 sites. Previous studies at the same sites found elevated ETR_{max} when comparing *P. pavonica* at an elevated CO_2 site compared to an ambient CO_2 site (Johnson et al., 2012). If the duration of our experiment had been longer, our transplanted *P. pavonica* may also have significantly increased their ETR_{max}. Our results emphasize the likelihood that ocean acidification will act upon primary production differently at different latitudes and depths, not always according to our expectations. This is important since increases in land nutrient run-off, due to changes in land use and/or rainfall, are altering light levels in coastal waters (Scherner et al., 2013).

One of the most important photoprotective mechanisms available to algae is an ability to dissipate excess thermal energy (Adams et al., 2006). Thermal dissipation measured as non-photochemical PSII fluorescence quenching (NPQ) is triggered by the trans-thylakoidal proton gradient (ΔpH) and zeaxanthin (ZEA) synthesis through the xanthophyll cycle (Gilmore et al., 1994) and is recognized as the most important photoprotective mechanisms in higher plants and several algal divisions (Rodrigues et al., 2002). Fucoxanthin and violaxanthin levels were not affected in *C. compressa* whereas in *P. pavonica* fucoxanthin and violaxanthin increased under 70%$_{PAB}$ conditions, nutrient enrichment and medium CO_2 levels. We used NPQ_{max} as an indicator of photoprotective energy dissipation efficiency (Celis-Plá et al., 2014b), and we also measured phenolic content and antioxidant activity (EC_{50}), both of which can be used as photoprotectors (Celis-Plá et al., 2014a). In *C. compressa* and *P. pavonica* NPQ_{max} was higher in all shaded treatments with nutrient enrichment, but not in the fully lit treatments, indicating higher photoprotection when nutrients were elevated and light was reduced. Phenols usually accumulated under higher irradiance and (for *C. compressa*) higher CO_2 treatments, as per past studies on kelp grown at high CO_2 (Swanson and Fox, 2007), or measured under higher irradiance (Connan et al., 2004). However, the effects of CO_2 on autotroph phenol production are not straight forward, as previous work has shown that both seagrass (Arnold et al., 2012) and the macroalga *Cystoseira tamariscifolia* (Figueroa et al., 2014b) decrease phenol production when CO_2 increased. In *C. compressa* and *P. pavonica*, antioxidant activity and EC_{50} were affected by the interactions between light levels and CO_2. EC_{50} tended to be higher in shaded, high CO_2

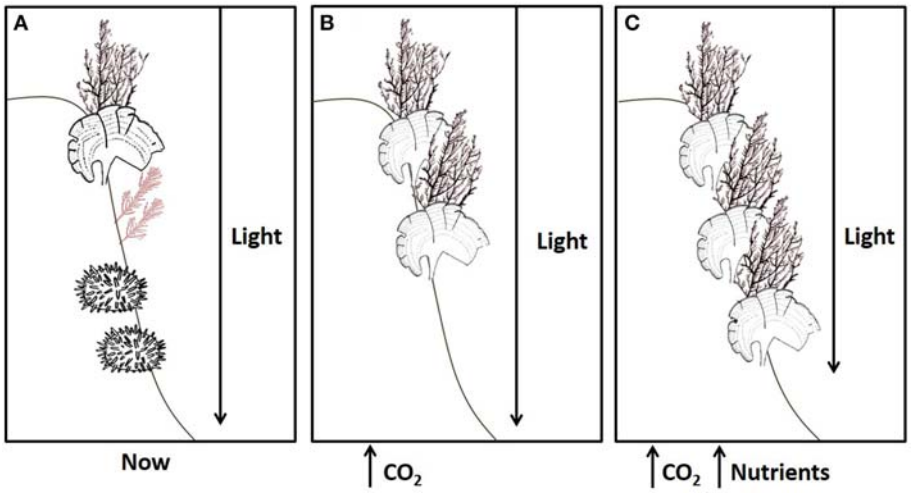

FIGURE 6 | The effects of ocean acidification on rocky shore communities will depend on nutrient levels. (A) A typical brown algal canopy with coralline algae and sea urchins at present-day levels of CO_2, nutrients and light. **(B)** Increased CO_2 in oligotrophic conditions has adverse impacts on most calcified organisms, such as coralline algae and sea urchins, yet dense brown algal stands persist at shallow depths despite corrosion of facultatively calcified algae, such as Padina. **(C)** Ocean acidification remains detrimental to most calcified organisms, but when this is combined with nutrient enrichment fleshy algae can flourish since they are able to take full advantage of increases in CO_2, extending deeper into the photic zone despite increased turbidity.

treatments with and without nutrient addition, suggesting a positive correlation with phenolic compounds and their use as antioxidants to prevent photodamage. Together, NPQ_{max}, phenol production and EC_{50} indicate that in elevated CO_2 conditions some species will have a higher capacity for photoprotection.

Macroalgae regulate their biochemical composition to changes in solar radiation (Bischof et al., 2006; Figueroa et al., 2014a,b). Whilst light obviously affects photosynthesis, other variables such pH, nutrients and the availability of different DIC species all have the potential to affect photosynthetic rates (Raven and Beardall, 2014). As interactions among such factors will determine the success of algal species and the amount of primary productivity in any time and place, it is crucial to know how the effects of ocean acidification are modified by other key drivers of photosynthesis. Research similar to our study, but with more species, in more locations and for longer durations, is clearly required before solid conclusions can be made with respect to the effects of ocean acidification on macroalgal productivity.

In conclusion, our study shows that ongoing ocean acidification can be expected to increase photosynthetic efficiency and algal productivity. The magnitude of these effects, and the species that benefit, will depend on light and nutrient levels. We show that *C. compressa* and *P. pavonica* are able to benefit from an increase in CO_2 levels, rapidly changing their physiology and biochemical composition over 3 day alterations in DIC, irradiance and nutrients. These factors had interactive effects on photosynthetic and photoprotective systems in both species and help explain why brown algae proliferate at CO_2 seeps. Longer-term growth studies involving algal interactions would be useful: we remain concerned that chronic eutrophication combined with ocean acidification may benefit more opportunistic algal groups to the detriment of canopy-forming brown macroalgae. As ocean acidification is not happening in isolation, but alongside a plethora of other anthropogenic changes, an understanding of the interactive effects of multiple stressors is critical to plan for global ocean change. We have shown that elevated CO_2 levels can enhance brown algal productivity, and may boost the kelp and fucoid forests of the planet, but the effects will depend upon interactions with other physicochemical parameters such as light and nutrient availability.

Acknowledgments

This work was supported by the Junta de Andalucía (Project RNM-5750) and by the research group RNM-295. The NERC/Defra/DECC UK Ocean Acidification research programme and Save Our Seas Foundation contributed to fieldwork expenses (this video https://vimeo.com/101795615 shows the field site). PC gratefully acknowledges financial support from "Becas-Chile" (CONICYT) fellowship of doctorate of the Ministry of Education of the Republic of Chile. P. A. Horta is also grateful to CNPq grants, CAPES (PNADB/visitant professor fellowship) and INCT-MC to additional financial support.

Supplementary Material

The Supplementary Material for this article can be found online at: http://journal.frontiersin.org/article/10.3389/fmars.2015.00026/abstract

References

Adams, W. W. I. I. I., Zarter, C. R., Mueh, K. E., Amiard, V. S. E., and Demmig-Adams, B. (2006). "Energy dissipation and photoinhibition: a continuum of photoprotection," in *Photoprotection, Photoinhibition, Gene Regulation, and Environment,* eds B. Demmig-Adams, W. W. III. Adams, A, Mattoo (Dordrecht: Springer), 49–64.

Aphalo, P. J., Albert, A., McLeod, A., Heikkilä, A., Gómez, I., Figueroa, F. L., et al. (2013). "2 Manipulating UV radiation," in *Beyond the Visible A Handbook of Best Practice in Plant UV Photobiology*, eds P. J. Aphalo, A. Albert, L. O. Björn, A. McLeod, T. M. Robson, and E. Rosenqvist (COST Action FA0906 UV4growth, Helsinki: University of Helsinki, Division of Plant Biology), 35–70.

Arnold, T., Mealey, C., Leahey, H., Miller, A. W., Hall-Spencer, J. M., Milazzo, M., et al. (2012). Ocean acidification and the loss of phenolic substances in marine plants. *PLoS ONE* 7:e35107. doi: 10.1371/journal.pone.0035107

Baggini, C., Salomidi, M., Voutsinas, E., Bray, L., Krasakopoulou, E., and Hall-Spencer, J. M. (2014). Seasonality affects macroalgal community response to increases in pCO_2. *PLoS ONE* 9:e106520. doi: 10.1371/journal.pone.0106520

Bermejo, R., De la Fuente, G., Vergara, J. J., and Hernández, I. (2013). Application of the CARLIT index along a biogeographical gradient in the Alboran Sea (European Coast). *Mar. Pollut. Bull.* 72, 107–118. doi: 10.1016/j.marpolbul.2013.04.011

Bischof, K., Gómez, I., Molis, M., Hanelt, D., Karsten, U., Lüder, U., et al. (2006). Ultraviolet radiation shapes seaweed communities. *Rev. Environ. Sci. Biot.* 5, 141–166. doi: 10.1007/s11157-006-0002-3

Blois, M. S. (1958). Antioxidant determinations by the use of a stable free radical. *Nature* 181, 1199–1200. doi: 10.1038/1811199a0

Boatta, F., D'Alessandro, W., Gagliano, A. L., Liotta, M., Milazzo, M., Rodolfo-Metalpa, R., et al. (2013). Geochemical survey of Levante Bay, Vulcano Island (Italy) and its suitability as a natural laboratory for the study of ocean acidification. *Mar. Pollut. Bull.* 73, 485–494. doi: 10.1016/j.marpolbul.2013.01.029

Brodie, J., Williamson, C., Smale, D. A., Kamenos, N. A., Mieszkowska, N., Santos, R., et al. (2014). The future of the northeast Atlantic benthic flora in a high CO_2 world. *Ecol. Evol.* 4, 2787–2798. doi: 10.1002/ece3.1105

Calosi, P., Rastrick, S. P. S., Graziano, M., Thomas, S. C., Baggini, C., Carter, H. A., et al. (2013). Distribution of sea urchins living near shallow water CO_2 vents is dependent upon species acid-base and ion-regulatory abilities. *Mar. Poll. Bull.* 73, 470–484 doi: 10.1016/j.marpolbul.2012.11.040

Celis-Plá, P. S. M., Korbee, N., Gómez-Garreta, A., and Figueroa, F. L. (2014b). Seasonal photoacclimation patterns in the intertidal macroalga *Cystoseira tamariscifolia* (Ochrophyta). *Sci. Mar.* 78, 377–388. doi: 10.3989/scimar.04053.05A

Celis-Plá, P. S. M., Martínez, B., Quintano, E., García-Sánchez, M., Pedersen, A., Navarro, N. P., et al. (2014a). Short-term ecophysiological and biochemical responses of *Cystoseira tamariscifolia* and *Ellisolandia elongata* to changes in solar irradiance and nutrient levels. *Aquat. Biol.* 22, 227–243. doi: 10.3354/ab00573

Connan, S., Goulard, F., Stiger, V., Deslandes, E., and Ar-Gall, E. (2004). Interspecific and temporal variation in phlorotannin levels in an assemblage of brown algae. *Bot. Mar.* 47, 410–416. doi: 10.1515/BOT.2004.057

Connell, S. D., Kroeker, K. J., Fabricius, K. E., Kline, D. I., and Russell, B. D. (2013). The other ocean acidification problem: CO_2 as a resource among competitors for ecosystem dominance. *Philos. Trans. R. Soc. Lond. B Biol. Sci.* 368:20120442. doi: 10.1098/rstb.2012.0442

Cornwall, C. E., Revill, A. T., and Hurd, C. L. (2015). High prevalence of diffusive uptake of CO_2 by macroalgae in a temperate subtidal ecosystem. *Photosynth. Res.* 124, 181–190. doi: 10.1007/s11120-015-0114-0

Dickson, A. G. (1990). Standard potential of the reaction: $AgCl(s) + 1/2\ H_2(g) = Ag(s) + HCl(aq)$, and the standard acidity constant of the ion HSO_4^- in synthetic seawater from 273.15 to 318.15 KJ. *J. Chem. Thermodyn.* 22, 113–127. doi: 10.1016/0021-9614(90)90074-Z

Eilers, P. H. C., and Peeters, J. C. H. (1988). A model for the relationship between light intensity and the rate of photosynthesis in phytoplankton. *Ecol. Model.* 42, 199–215. doi: 10.1016/0304-3800(88)90057-9

Falkenberg, L. J., Connell, S. D., and Russell, B. D. (2013). Disrupting the effects of synergies between stressors: improved water quality dampens the effects of future CO_2 on a marine habitat. *J. Appl. Ecol.* 50, 51–58. doi: 10.1111/1365-2664.12019

Ferreira, J. G., Andersen, J. H., Borja, A., Bricker, S. B., Camp, J., Cardoso da Silva, M., et al. (2011). Overview of eutrophication indicators to assess environmental status within the European Marine Strategy Framework Directive. *Estuar. Coast. Shelf. S.* 93, 117–131. doi: 10.1016/j.ecss.2011.03.014

Figueroa, F. L., Conde-Álvarez, R., and Gómez, I. (2003). Relations between electron transport rates determined by pulse amplitude modulated chlorophyll fluorescence and oxygen evolution in macroalgae under different light conditions. *Photosynth. Res.* 75, 259–275. doi: 10.1023/A:1023936313544

Figueroa, F. L., Dominguez-González, B., and Korbee, N. (2014a). Vulnerability and acclimation to increased UVB in the three intertidal macroalgae of different morpho-functional groups. *Mar. Env. Res.* 101, 8–21. doi: 10.1016/j.marenvres.2014.01.009

Figueroa, F. L., Malta, E.-J., Bonomi-Barufi, J., Conde-Álvarez, R., Nitschke, U., and Arenas, F. (2014b). Short-term effects of increasing CO_2, nitrate and temperature on three Mediterranean macroalgae: biochemical composition. *Aquat. Biol.* 22, 177–193. doi: 10.3354/ab00610

García-Plazaola, J. I., and Becerril, J. M. (1999). A rapid HPLC method to measure lipophilic antioxidants in stressed plants: simultaneous determination of carotenoids and tocopherols. *Phytochem. Anal.* 10, 307–313.

García-Plazaola, J. I., Fernandez-Marin, B., and Porcar-Castell, A. (2012). Thermal energy dissipation and xanthophyll cycles beyond the Arabidopsis model. *Photosynth. Res.* 113, 89–103. doi: 10.1007/s11120-012-9760-7

Gaylord, B., Kroeker, K. J., Sunday, J. M., Anderson, K. M., Barry, J. P., Brown, N. E., et al. (2015). Ocean acidification through the lens of ecological theory. *Ecology* 96, 3–15. doi: 10.1890/14-0802.1

Gilmore, A. M., Mohanty, N., and Yamamoto, H. Y. (1994). Epoxidation of zeaxanthin and antheraxanthin reverses non-photochemical quenching of photosystem II chlorophyll a fluorescence in the presence of trans-thylakoid DpH. *FEBS. Lett.* 390, 271–274. doi: 10.1016/0014-5793(94)00784-5

Giordano, M., Beardall, J., and Raven, J. A. (2005). CO_2 concentrating mechanisms in algae: mechanisms, environmental modulation, and evolution. *Annu. Rev. Plant Biol.* 56, 99–131. doi: 10.1146/annurev.arplant.56.032604.144052

Hanelt, D., and López-Figueroa, F. (2012). "Physiological and photomorphogenic effects of light of marine macrophytes," in *Seaweed Biology Ecological Studies,* eds C. Wienke and K. Bischof (Verlag: Springer), 3–23. doi: 10.1007/978-3-642-28451-9_1

Harley, C. D. G., Anderson, K. M., Demes, K. W., Jorve, J. P., Kordas, R. L., and Coyle, T. A. (2012). Effects of climate change on global seaweed communities. *J. Phycol.* 48, 1064–1078. doi: 10.1111/j.1529-8817.2012.01224.x

Hepburn, C. D., Pritchard, D. W., Cornwall, C. E., Mcleod, R. J., Beardall, J., Raven, J. A., et al. (2011). Diversity of carbon use strategies in a kelp forest community: implications for a high CO_2 ocean. *Glob. Chan. Biol.* 17, 2488–2497. doi: 10.1111/j.1365-2486.2011.02411.x

Hofmann, L. C., Heiden, J., Bischof, K., and Teichberg, M. (2014). Nutrient availability affects the response of the calcifying chlorophyte Halimeda opuntia (L.) J.V. Lamouroux to low pH. *Planta* 239, 231–242. doi: 10.1007/s00425-013-1982-1

Hurd, C. L., Harrison, P. J., Bischof, K., and Lobban, C. S. (2014). *Seaweed Ecology and Physiology, 2nd Edn.* Cambridge: Cambridge University Press.

Johnson, V. R., Russell, B. D., Fabricius, K. E., Brownlee, C., and Hall-Spencer, J. M. (2012). Temperate and tropical brown macroalgae thrive, despite decalcification, along natural CO_2 gradients. *Glob. Chan. Biol.* 18, 2792–2803. doi: 10.1111/j.1365-2486.2012.02716.x

Koch, M., Bowes, G., Ross, C., and Zhang, X. (2013). Climate change and ocean acidification effects on seagrasses and marine macroalgae. *Glob. Chan. Biol.* 19, 103–132. doi: 10.1111/j.1365-2486.2012.02791.x

Koroleff, F. (1983). "Determination of phosphorus," in *Methods of Seawater Analysis: Second, revised and extended edition,* eds K. Grasshoff, M. Ehrhardt, K. Kremling (Weinheim: Verlag Chemie), 125–139.

Martínez, B., Arenas, F., Rubal, M., Burgués, S., Esteban, R., García-Plazaola, I., et al. (2012). Physical factors driving intertidal macroalgae distribution: physiological stress of a dominant fucoid at its southern limit. *Oecologia* 170, 341–353. doi: 10.1007/s00442-012-2324-x

Oviedo, A. M., Ziveri, P., Álvarez, M., and Tanhua, T. (2015). Is coccolithophore distribution in the Mediterranean Sea related to seawater carbonate chemistry? *Ocean Sci. Discuss.* 11, 613–653. doi: 10.5194/osd-11-613-2014

Pérez-Lloréns, J. L., Vergara, J. J., Pino, R. R., Hernandez, I., Peralta, G., and Niell, F. X. (1996). The effect of photoacclimation on the photosynthetic physiology of *Ulva curvata* and *Ulva rotun data* (Ulvales, Chlorophyta). *Eur. J. Phycol.* 31, 349–359. doi: 10.1080/09670269600651581

Pettit, L. R., Smart, C. W., Hart, M. B., Milazzo, M., and Hall-Spencer, J. M. (2015). Seaweed fails to prevent ocean acidification impact on foraminifera along a shallow-water CO_2 gradient. *Ecol. Evol.* 5, 1784–1793. doi: 10.1002/ece3.1475

Pierangelini, M., Stojkovic, S., Orr, P. T., and Beardall, J. (2014). Elevated CO_2 causes changes in the photosynthetic apparatus of a toxic cyanobacterium, *Cylindrospermopsis raciborskii*. *J. Plant Physiol.* 171, 1091–1098. doi: 10.1016/j.jplph.2014.04.003

Pierrot, D. E., and Wallace, D. W. R. (2006). *MS Excel Program Developed for CO_2 System Calculations. ORNL/CDIAC-105a. Carbon Dioxide Information Analysis Center*, *Oak Ridge National Laboratory.* Oak Ridge, TN: U.S. Department of Energy.

Porzio, L., Buia, M. C., and Hall-Spencer, J. M. (2011). Effects of ocean acidification on macroalgal communities. *J. Exp. Mar. Biol. Ecol.* 400, 278–287. doi: 10.1016/j.jembe.2011.02.011

Raven, J. A., and Beardall, J. (2014). CO_2 concentrating mechanisms and environmental change. *Aquat. Bot.* 118, 24–37. doi: 10.1016/j.aquabot.2014.05.008

Raven, J. A., Beardall, J., and Giordano, M. (2014). Energy costs of carbon dioxide concentrating mechanisms in aquatic organisms. *Photosynth. Res.* 121, 111–124. doi: 10.1007/s11120-013-9962-7

Rodrigues, M. A., Dos Santos, C. P., Young, A. J., Strbac, D., and Hall, D. O. (2002). A smaller and impaired xanthophyll cycle makes the deep sea macroalgae *Laminaria abyssalis* (Phaeophyceae) highly sensitive to daylight when compared with shallow water *Laminaria digitata*. *J. Phycol.* 38, 939–947. doi: 10.1046/j.1529-8817.2002.t01-1-01231.x

Roleda, M. Y., Morris, J. N., McGraw, C. M., and Hurd, C. L. (2012). Ocean acidification and seaweed reproduction: increased CO_2 ameliorates the negative effect of lowered pH on meiospore germination in the giant kelp *Macrocystis pyrifera* (Laminariales, Phaeophyceae). *Glob. Chan. Biol.* 18, 854–864. doi: 10.1111/j.1365-2486.2011.02594.x

Roy, R. N., Roy, L. N., Vogel, K. M., Porter-Moore, C., Pearson, T., Good, C. E., et al. (1993). The dissociation constants of carbonic acid in seawater at salinities 5 to 45 and temperatures 0 to 45° C. *Mar. Chem.* 4, 249–267. doi: 10.1016/0304-4203(93)90207-5

Russell, B. D., Pasasrelli, C. A., and Connell, S. D. (2011). Forecasted CO_2 modifies the influence of light in shaping subtidal habitat. *J. Phycol.* 47, 744–752. doi: 10.1111/j.1529-8817.2011.01002.x

Russell, B. D., Thompson, J. I., Falkenberg, L. J., and Connell, S. D. (2009). Synergistic effects of climate change and local stressors: CO_2 and nutrient-driven change in subtidal rocky habitats. *Glob. Chan. Biol.* 15, 2153–2162. doi: 10.1111/j.1365-2486.2009.01886.x

Scherner, F., Horta, P. A., Oliveira, E. C., Simonassi, J. C., Hall-Spencer, J. M., Chow, F., et al. (2013). Coastal urbanization leads to remarkable seaweed species loss and community shifts along the SW Atlantic. *Mar. Poll. Bull.* 76, 106–115. doi: 10.1016/j.marpolbul.2013.09.019

Schreiber, U., Endo, T., Mi, H., and Asada, K. (1995). Quenching analysis of chlorophyll fluorescence by the saturation pulse method: particular aspects relating to the study of eukaryotic algae and cyanobacteria. *Plant Cell. Physiol.* 36, 873–882.

Strain, E. M. A., Thomson, R. J., Micheli, F., Mancuso, F. P., and Airoldi, L. (2014). Identifying the interacting roles of stressors in driving the global loss of canopy-forming to mat-forming algae in marine ecosystems. *Glob. Chan. Biol.* 20, 3300–3312. doi: 10.1111/gcb.12619

Swanson, A. K., and Fox, C. H. (2007). Altered kelp (Laminariales) phlorotannins and growth under elevated carbon dioxide and ultraviolet-B treatments can influence associated intertidal food webs. *Glob. Chan. Biol.* 13, 1696–1709. doi: 10.1111/j.1365-2486.2007.01384.x

Yesson, C., Bush, L. E., Davies, A. J., Maggs, C. A., and Brodie, J. (2015). Large brown seaweeds of the British Isles: evidence of changes in abundance over four decades. *Estuar. Coast. Shelf. S.* 155, 167–175. doi: 10.1016/j.ecss.2015.01.008

Zou, D., and Gao, K. (2009). Effects of elevated CO_2 on the red seaweed *Gracilaria lemaneiformis* (Gigartinales, Rhodophyta) grown at different irradiance levels. *Phycologia* 48, 510–517. doi: 10.2216/08-99.1

Conflict of Interest Statement: The authors declare that the research was conducted in the absence of any commercial or financial relationships that could be construed as a potential conflict of interest.